Two-stage Atomic Layer Deposition of Smooth Aluminum Oxide on Hydrophobic Self-assembled Monolayers

Nobuhiko P. Kobayashi and R. Stanley Williams

Abstract— **We describe the growth of aluminum oxide (AlOx) on strong hydrophobic surfaces that consist of CH3-terminated self-assembled monolayers (CH_3-SAMs) by utilizing atomic layer deposition (ALD) with H_2O as the oxygen source. The evolution of AlO_x on the CH_3-SAMs was studied by comparing with that on hydrophilic OH-terminated silicon dioxide (OH-SiO_2). The AlO_x grown on the CH_3-SAM surfaces underwent growth instability and developed significantly rough surface morphologies while the AlO_x on the OH-SiO_2 maintained atomically smooth surface morphologies. The structural integrity of the CH_3-SAMs was also found to be disturbed substantially at the onset of the ALD process with H_2O. In order to improve the surface morphology of AlO_x on CH_3-SAM surfaces, a two-stage ALD process was developed. In the two-stage ALD process for AlO_x, the first stage utilized n-propanol as the oxygen source and the second stage proceeded with H_2O. The optimized two-stage ALD process significantly improved the surface morphology of AlO_x films and effectively protected the structural integrity of underlying CH_3-SAMs.**

***Index Terms*—atomic layer deposition, aluminum oxide, self-assembled monolayer, surface morphology**

I. Introduction

In optimizing functional devices in which organic materials are used as active components, employing encapsulation films that shield organic materials during processing and effectively prevent water and oxygen from penetrating into organic materials during device operation is often desirable. Although the formation of organic films on inorganic substrates (i.e. organic on inorganic) has been studied extensively in the development of functional organic devices [1-3], detailed studies on the deposition of inorganic films onto organic layers (i.e. inorganic on organic) are still limited to a few reports on metal oxides / nitrides [4-7] and elementary metals [8-10] deposited on self-assembled monolayers (SAMs). In this paper, we describe the growth of aluminum oxide (AlO_x) on CH_3-terminated SAMs (hydrophobic surfaces), i.e. inorganic on organic, at low temperatures. Our objective is to study the growth of an inorganic film on organic layers in the context of developing an encapsulation layer that can cover organic layers uniformly at low temperatures. We utilize a deposition process such as atomic layer deposition (ALD) at low temperatures so that organic layers are not chemically and physically disturbed. This paper consists of two parts. First, a comparative study of a conventional ALD process using H_2O as the oxygen source on hydrophobic and hydrophilic surfaces is described. In the conventional ALD process, as the nominal thickness of the AlO_x films increases, the films on the CH_3-SAM exhibited a growth instability accompanied with a rough surface morphology, while the films on the OH-SiO_2 maintained an atomically smooth surface. And then, we attempted to control surface wettability in the early stage of ALD processes. In the attempt, AlO_x was deposited onto hydrophobic CH_3-SAM surfaces by a newly developed two-stage ALD process in which the first stage utilized n-propanol as the oxygen source and the second stage proceeds with water.

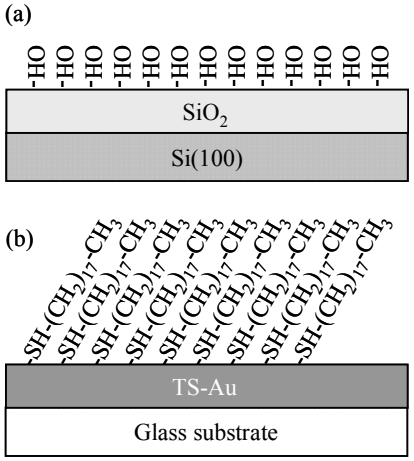

Figure 1. Schematics show two types of substrates on which AlO_x was deposited. (a) OH-SiO_2 and (b) CH_3-SAMs.

Manuscript received August 17, 2007.

N. P. Kobayashi is with Baskin School of Engineering at University of California Santa Cruz, Santa Cruz, CA 95064 USA (phone: 831-459-3571; e-mail: nobby@soe.ucsc.edu) and Nanostructured Energy Conversion Technology and Research (NECTAR), Advanced Studies Laboratories, University of California Santa Cruz and NASA Ames Research Center, Moffett Field, CA 64035 USA.

R. S. Williams is with Information and Quantum Systems Laboratory at Hewlett-Packard Laboratories, Palo Alto, CA 94034 USA (e-mail: stan.williams@hp.com).

(Advance online publication: 20 May 2008)

II. Substrate Preparation

Shown schematically in Fig. 1(a) and (b) are two types of substrates, representing hydrophilic and hydrophobic surfaces, respectively, used in this study. On these two types of substrates having different characteristics of wettability, AlO_x was deposited by ALD to study how the growth of AlO_x progressed on different surfaces. Panel (a) represents a hydrophilic surface provided by a hydroxyl terminated silicon dioxide surface ($OH\text{-}SiO_2$). The silicon dioxide was thermally grown on a silicon (100) surface by a standard high temperature oxidation process used in complementary metal-oxide-semiconductor (CMOS) processes.

Panel (b) represents a hydrophobic surface provided by CH_3-terminated self-assembled monolayers (CH_3-SAMs). In preparing the CH_3-SAM surfaces, first a gold film with an atomically smooth surface was prepared on glass substrates via our template-stripping process [11]. Subsequently SAMs of the alkanethiolate $CH_3\text{-}(CH_2)17SH$ were formed on the template-stripped gold (TS-gold) film by immersion into an ethanol solution containing the alkanethiolate at a molar concentration of 0.01 M/l for 24 hours at room temperature. The TS-gold surface having atomically smooth surface profiles ensures that CH_3-SAMs are formed with minimum number of structural defects, resulting in atomically smooth surface morphologies. The CH_3-SAM surface is expected to be strongly hydrophobic manifested in the early stage of the deposition of AlO_x for which H_2O is used as a source of oxygen.

A. Conventional Atomic Layer Deposition Process

AlO_x films were deposited by conventional atomic layer deposition (ALD), using H_2O and trimethylaluminum (TMAl) as sources for oxygen and aluminum respectively. The ALD process was performed by alternatively supplying pulses of nitrogen gas containing either H_2O or TMAl vapor. A set of key deposition parameters are listed in Table I. The substrate temperature was set to 45 °C for all samples, which was lower than those temperatures reported to cause SAMs to degrade structurally [12]. Dissociative reaction, including ligand exchange, of TMAl on SAMs with CH_3 functional group has been found to be nearly quenched due to the small thermodynamic driving force and large kinetic barrier [6], however as mentioned earlier, our primary objective was to study the deposition of AlO_x on SAMs at low temperature to form a protective barrier that does not disrupt the SAM during deposition, and thus the relative inertness of TMAl on CH_3-SAMs was, in fact, a potential advantage. In addition, H_2O

Temperature	45°C
Sources	$Al(CH_3)_3$ and H_2O
Chamber base pressure	~2x10-1 torr
H_2O purge	140 ms,
H_2O purge	160 s
$Al(CH_3)_3$ pulse	140 ms
$Al(CH_3)_3$ purge	16 s
Deposition rate	0.12 nm/cycle

Table I. Deposition parameters of a conventional ALD process using H_2O.

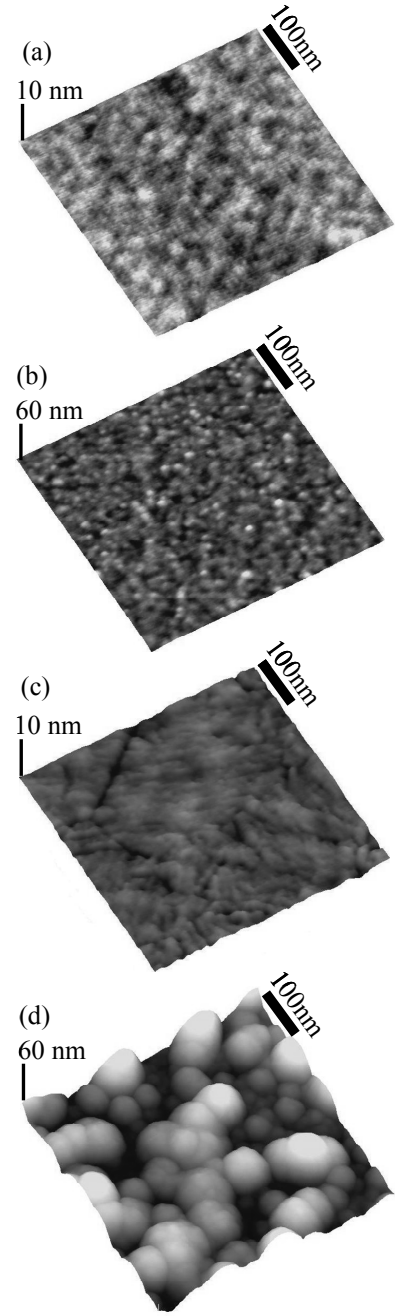

Figure 2. AFM images collected on (a) as-formed $OH\text{-}SiO_2$, (b) 400-ALD cycle AlOx on the $OH\text{-}SiO_2$, (c) as-formed CH_3-SAMs, and (d) 400-ALD cycle AlO_x on the CH_3-SAMs.

used as the oxygen source is not reactive with alkane chains in the SAMs, thus the CH_3-SAMs were expected to favor the formation of water droplets on the surface of the densely packed SAMs that enabled pyrophoric TMAl to dissociate and form AlO_x nuclei on the surface of the CH_3-SAMs.

One cycle of the ALD process consists of a 140 ms water pulse followed by a 160 s nitrogen purge period, after that, a 140 ms TMAl pulse was given and followed by another 16s nitrogen purge period. This specific deposition conditions were previously optimized for AlO_x at 45 °C, and confirmed to maintain a deposition rate of self-limited 0.12 nm/cycle on an OH-terminated silicon surfaces, which ensured a precise and reproducible amount of source materials to be delivered to the SAM surface during the ALD process.

B. Comparison of Aluminum Oxide Deposited by Conventional ALD

Fig. 2 show representative non-contact mode AFM images collected on the AlO_x deposited on the OH-SiO_2 in (a)(b) and on the CH_3-terminated SAM in (c)(d) for the 0, and 400 ALD cycle samples, respectively. As shown in (a) as-prepared OH-SiO_2 surface exhibits an atomically smooth surface morphology and, as seen in (b), the surface morphology of the AlO_x on the OH- SiO_2 surface essentially maintained the atomically smooth surface morphology with slight increases in root-mean-square roughness (Rrms) from 0.11 nm to 0.37 nm. As seen in Fig. 2(c), the surface of the freshly prepared CH_3-SAM exhibited atomically smooth morphology with Rrms of 0.24 nm. However, Rrms increased significantly to 8.09 nm after 400 ALD cycles was completed as seen in (d). The rough surface developed during the 400 cycles of ALD appears to be covered with granular-like surface features separated by voids.

Shown in Fig. 3 are water contact angle (θ_{cont}) measurements on the surfaces of AlO_x on the CH_3-SAM (solid red circles) and the OH-SiO_2 (solid blue triangles). On the CH_3-SAM, the water contact angle on the surface of freshly prepared alkanethiol SAMs was approximately 106 degree, indicating high-quality SAM. Once AlO_x was deposited on the CH_3-SAM, the water contact angle decreased steadily as the thickness increased until the thickness reached 25-30 nm. Subsequently, the water contact angle appeared to increase slowly. In contrast, the water contact angle on the SiO_2 remained nearly unchanged from the initial number for the 0 ALD cycle sample. The gradual decrease in the water contact angle on the CH_3-SAM suggests that the surface of the CH_3-SAM is not uniformly covered with AlO_x, as indicated by the AFM image in Fig. 2(d).

Reflection absorption infrared spectroscopy spectra (RAIRS) collected from the AlO_x sample after 200 ALD cycles is shown in Fig. 4 (spectrum (a)) with a reference RAIRS spectrum collected from freshly-prepared CH_3-SAM (spectrum (b)). In the reference spectrum, the four peaks that are well-resolved and numbered 1 - 4 are associated with asymmetric CH_3 (a-CH_3), asymmetric CH_2 (a-CH_2), symmetric CH_3 (s-CH_3), and symmetric CH_2 (s-CH_2) stretching modes, respectively, suggesting that the CH_3-SAM was well-ordered on the TS-Au surface. The RAIRS spectrum collected on the 200-cycle ALD sample showed significant contrast to the reference spectrum. The CH_3 peaks (peaks 1 and 3) disappeared completely, implying that the CH_3 functional group of the SAMs experienced a substantial perturbation as a result of the AlO_x deposition. As mentioned earlier, the reaction of TMA with CH_3-SAMs was found to form no adsorbed complex and the ligand exchange reaction to form methane needs to go through a large kinetic energy barrier [17]. In contrast to the instantaneous disappearance of the CH_3 peaks, the CH_2 peaks were found to be present even on the 200-ALD cycle sample. The CH_2 peak (peaks 2 and 4) were still present, however they were substantially perturbed. Both peak 2 and

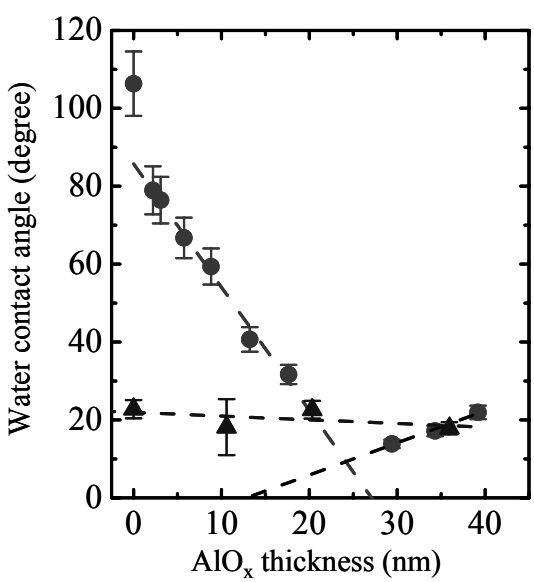

Figure 3. Plot of water contact angle on the surfaces of the AlO_x on the hydrophobic CH_3-SAM surfaces (solid circles) and the hydrophilic OH-SiO_2 surfaces (solid triangles).

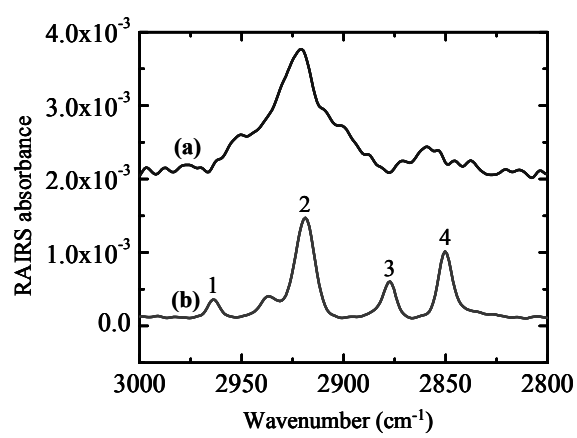

Figure 4. RAIRS spectra collected from AlO_x samples after 200-ALD cycles on the CH_3-SAMs (a). The spectrum (b) is a reference collected from as-formed CH_3-SAMs without AlOx deposition.

peak 4 showed significant broadening and peak shifts. Both a-CH_2 and s-CH_2 mode peaks exhibited significant broadening and peak shift even after only 25-ALD cycles (not shown), suggesting that the ALD process in the early stages of the deposition (upto 25 PFD cycles) resulted in the formation of structural disorder within the alkane chains of the SAMs.

The AFM and the RAIRS results, in the comparison of the way AlO_x evolves on the CH_3-SAMs (hydrophobic) and OH-SiO_2 (hydrophilic) surfaces, clearly suggests that it is the wetting characteristics of H_2O pulses in the early stage of the deposition that dictates the surface morphology of the AlO_x in the later stage. On CH_3-SAMs, numerous small water droplets would form during H_2O pulses, and TMA is expected to react spontaneously with these water droplets pre-existing on the CH_3-SAMs surface. Clearly, atomic-scale studies on the early stage of the AlO_x deposition on CH_3-terminated SAMs need to be done to address several questions raised in our experiment such as the physical and/or chemical origin of the results that the CH_3 vibration modes disappeared and the CH_2 vibration modes broadened significantly at the onset of the ALD process.

III. Two-stage Atomic Layer Deposition

A. *n-propanol as an Oxygen Source*

The growth instability observed in the evolution of AlO_x films on the CH_3-SAMs, in contrast to those on the OH-terminated SiO_2, eventually resulted in rough surface morphologies. The comparative studies on the CH_3-SAMs (hydrophobic) and the OH-SiO_2, (hydrophilic) surfaces suggested that the instability be associated with the characteristics of surface wetting by H_2O in a conventional ALD process, presumably in the early stages. In other words, deposition kinetics on hydrophobic surfaces in the early stage of ALD processes could be actively modified by adding chemical species that promote surface wetting by water on hydrophobic surfaces. Therefore, we examined the wetting properties of a mixture of water and *n*-propanol, instead of pure water, on the CH_3-SAMs.

Fig. 5 shows the contact angles measured at room temperature with a mixture of water and *n*-propanol on the CH_3-SAMs and plotted as a function of the volume percentage of *n*-propanol in the mixture (R). The contact angle sharply dropped within the range of R = 0-30 % and slowly saturated to θ approximately 43 degree afterward. The wetting characteristics progressively improved until R reached roughly 40 %, which suggests that utilizing *n*-propanol would improve surface morphology of AlO_x films on hydrophobic surfaces such as CH_3-SAMs during ALD processes. Clearly this new concept in ALD process at low temperatures would benefit other materials deposited on hydrophobic surfaces. Given the contact angle data, we attempted to explicitly control the surface wettability on the CH_3-SAM by utilizing *n*-propanol, instead of water, as the oxygen source in the early stage of a deposition. The vapor pressure and the heat of vaporization of *n*-propanol at 25 °C are comparable to those of water.

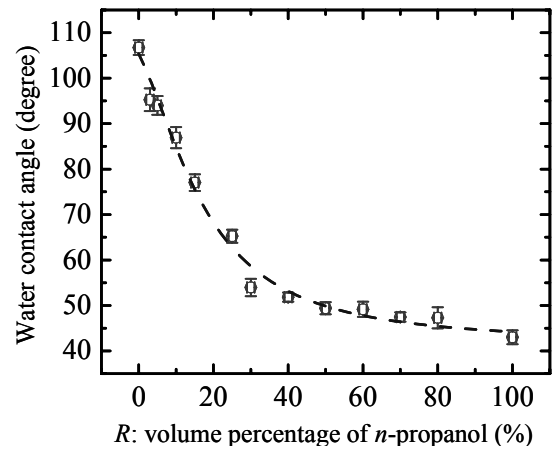

Figure 5. Contact angles measured on the CH_3-SAMs using a mixture of water and *n* -propanol with various concentration of *n*-propanol are plotted.

B. *Two-stage Atomic Layer Deposition Process*

In the two-stage atomic layer deposition process proposed here, we utilized pure *n*-propanol as the oxygen source to nucleate AlO_x on the CH_3-SAM in the first stage. Subsequently, in the second stage, H_2O was used as the oxygen source to further deposit AlO_x. In both stages, trimethylaluminum (TMAl) was used as the aluminum source. One ALD cycle in the initial stage was performed by supplying a 140 ms *n*-propanol pulse, a 160 s nitrogen purge period, a 140 ms TMAl pulse, and a 16 s nitrogen purge period. In the second stage, one cycle was performed in the same sequence using water instead of *n*-propanol. These specific deposition conditions were calibrated for AlO_x on OH-terminated silicon surfaces at 45 °C in order to maintain deposition rates self-limited at 0.02 and 0.08 nm / cycle in an *n*-propanol and a water ALD stage, respectively. All samples described below were identified by the cycle fraction $R_c = N_{n\text{-}propanol} / (N_{n\text{-}propanol} + N_{water})$, where $N_{n\text{-}propanol}$ and N_{water} are the total number of ALD cycles in an *n*-propanol (i.e. the first stage) and a water stage (i.e. the second stage), respectively. The substrate temperature was set to 45 °C for all samples to minimize structural damage on the CH_3-SAMs. The total number of pulses utilized was adjusted for each R_c to produce the same total film thickness from each deposition. Nominal (average) thicknesses of the AlO_x films measured by spectroscopic ellipsometry on all samples were within 31 ± 1 nm. In Table II, a set of key deposition parameters are listed.

C. *Comparison of Aluminum Oxide Deposited by the Two-stage ALD*

Show in Fig. 6 are representative AFM images (scan area of 500 x 500 nm) collected from AlO_x samples with (a) R_c = 0.002 (11 nm r.m.s. roughness) and (b) R_c = 0.301 (2.4 nm r.m.s. roughness). The r.m.s. roughness of the AlO_x films was found to be a strong function of R_c, which revealed a clear minimum in R_c within the range of $0.2 < R_c < 0.4$. Panel (a) reveals the similar morphological characteristics to those seen in Fig. 2(d), which reflects the fact that the sample with R_c = 0.002 was

First stage (*n*-propanol stage)		Second stage (H_2O stage)	
Temperature	45°C	Temperature	45°C
Sources	$Al(CH_3)_3$ and n-propanol	Sources	$Al(CH_3)_3$ and H_2O
Chamber base pressure	~2x10-1 torr	Chamber base pressure	~2x10-1 torr
n-propanol pulse	140 ms,	H_2O pulse	140 ms,
n-propanol purge	160 s	H_2O purge	160 s
$Al(CH_3)_3$ pulse	140 ms	$Al(CH_3)_3$ pulse	140 ms
$Al(CH_3)_3$ purge	16 s	$Al(CH_3)_3$ purge	16 s
Deposition rate	0.02 nm/cycle	Deposition rate	0.08 nm/cycle

$$R_c = N_{n\text{-}prop}/(N_{n\text{-}prop} + N_{water})$$

Table II. Deposition parameters of the two-stage ALD process

deposited with only one *n*-propanol ALD cycle and effectively identical to the sample represented in Fig. 2(d). The rough surface seen in (a) consists of multiple granules with a diameter and a height in the range of 43 nm and 12 nm, respectively. Several voids are also clearly seen. In contrast, the surface morphology shown in (b) is characterized by much smaller granules densely covering the surface and leaving a smaller number of voids, accounting for the smaller r. m. s. roughness on the surface of the sample with $R_c = 0.301$.

RAIRS measurement further revealed striking differences between the two samples discussed in Fig. 6. Fig. 7 are RAIRS spectra collected from the AlO_x samples with $R_c = 0.002$ (blue lines) and 0.301 (red lines), respectively. Since the absolute absorbance of RAIRS spectrum is highly sensitive to total structural characteristics of each sample, the absorption peaks of each spectrum were normalized with respect to the absorbance of the asymmetric CH_2 peak, i.e. peak 2 of each spectrum. Four peaks 1-4 seen in spectrum (a) represent asymmetric CH_3, asymmetric CH_2, symmetric CH_3, and symmetric CH_2 stretching modes, respectively. For the R_c = 0.301 sample (in red), the well-resolved spectrum indicates that the characteristics of the as-formed CH_3-SAM were well preserved. The peak positions of peaks 2 and 4 revealed no discernible peak shift with respect to the corresponding peak positions for the as-formed SAM, which further indicates that the alkyl chains were still well-ordered. A broadened shoulder on the lower wavenumber side of peak 2 is an indication of slight mode-softening within the alkyl chains [13]. The position of peaks 1 (2954.4 cm^{-1}) and 3 (2849.3 cm^{-1}) were shifted

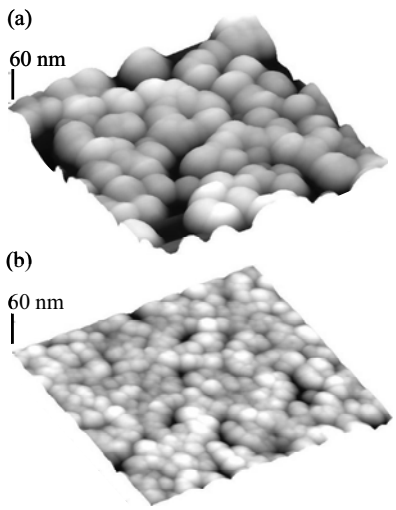

Figure 6. AFM images collected on R_c = (a) 0.002 and (b) 0.301 samples are shown. Each image is 500 x 500 nm scan.

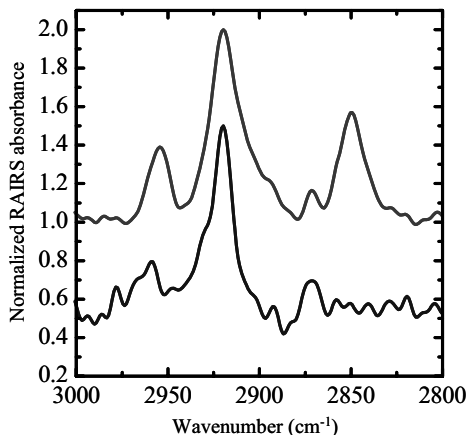

Figure 7. RAIRS spectra collected from R_c = 0.002 (bottom spectrum) and 0.301 (top spectrum) samples are shown. Four peaks shown are associated with C-H stretching modes for the CH_3-SAMs underneath the AlO_x films.

toward lower wavenumbers compared to those for the as-formed SAM (2964.1 and 2850.3 cm^{-1}), which indicates mode-softening of the terminal methyl groups [14]. The spectrum of the $R_c = 0.002$ sample reveals that all the vibration modes were strongly perturbed by the AlO_x deposition. Although peak 2 was still well-resolved, peak 4 was completely absent, which could be attributed to symmetry-breaking in the alkyl chains [15]. In addition, peak 1 appears to consist of two small peaks, suggesting the presence of both in-plane and out-of-plane asymmetric vibrational modes of CH_3 [16]. For the $R_c = 0.002$ sample, the RAIRS peaks were consistent with our previous observations for AlO_x deposition with water only [17].

The two stage ALD with $0.2 < R_c < 0.4$ process produced dramatically superior results compared to the growth using either water or *n*-propanol as the sole oxygen source for 31 nm AlO_x films. As indicated by the data of Fig. 5, the wettability of the CH_3-SAM surfaces increased substantially when pure *n*-propanol was used as the oxygen source, which significantly improved the surface roughness of the AlO_x during the initial stages of film growth. A major unanticipated bonus was that the CH_3-SAM was much less perturbed by the two stage AlO_x deposition, as shown by the RAIRS spectrum in Fig. 7 for $R_c = 0.301$ for which the r.m.s. roughness was minimum coincidently. One possibility for the improvement in the film roughness for $0.2 < R_c < 0.4$ could be that the wettability of a thin AlO_x film deposited with *n*-propanol is better for water than for *n*-propanol. However, we performed contact angle measurements on a 14 nm thick AlO_x film deposited only by *n*-propanol (corresponding to the $R_c = 0.826$ sample), and found that the contact angles for *n*-propanol and water were approximately 15° and 29.4°, respectively. Thus, there is some other driving force for the film roughening at $R_c = 0.826$, which may be the increasing incorporation of carbon into the growing film with thickness.

IV. Summary

The deposition of AlO_x on CH_3-SAMs (hydrophobic) and OH-SiO_2 (hydrophilic) surfaces by ALD were studied. During a conventional ALD using H_2O as an oxygen source, the AlO_x on CH_3-SAMs was found to undergo growth instability and develop substantially rough surface morphologies, which were attributed to the inefficient surface wetting on the hydrophobic CH_3-SAMs by H_2O in the early stage of the ALD. In the optimized two-stage ALD, using *n*-propanol in the first stage improved the surface morphology of AlO_x significantly and maintained the structural integrity of underlying CH_3-SAMs, suggesting the importance of explicitly controlling surface wetting in the early stage of a ALD process, in particular, on hydrophobic surfaces.

References

[1] C. D. Dimitrakopoulos and D. J. Mascaro, "Organic thin-film transistors: A review of recent advances," IBM J. Res. & Dev. **45**, 11 (2001).

[2] R. Toniolo and I. A. Hümmelgen, "Simple and fast organic device encapsulation using polyisobutene," Macromol. Mater. Eng. 289, 311 (2004).

[3] K. Morii, M. Ishida, T. Takashima, T. Shimoda, Q. Wang, Md. K. Nazeeruddlin, and M. Grätzel, "Encapsulation-free hybrid organic-inorganic light-emitting diodes, "Appl. Phys. Lett. 89, 183510 (2006).

[4] H. Shin, R. J. Collins, M. R. De Guire, A. H. Heuer, C. N. Sukenik, "Synthesis and characterization of TiO2 thin films on organic self-assembled monolayers: Part I. Film formation from aqueous solutions," J. Mater. Res. 10, 692 (1995).

[5] P. Wohlfart, J. Weiβ, J. Käshammer, M. Kreiter, C. Winter, R. Fisher, S. Mittler-Neher, "MOCVD of Aluminum Oxide/Hydroxide onto Organic Self-Assembled Monolayers," Chem. Vap. Deposition 5, 165 (1999).

[6] Y. Xu and C. B. Musgrave, "A DFT study of the Al2O3 atomic layer deposition on SAMs: effect of SAM termination," Chem. Mater. 16, 646 (2004).

[7] J. P. Lee, Y. J. Jang, M. M. Sung, "Atomic layer deposition of TiO2 thin films on mixed self-assembled monolayers studied as a function of surface free energy," Adv. Funct. Mater. 13, 873 (2003).

[8] A. Hooper, G. L. Fisher, K. Konstadinidis, D. Jung, H. Nguyen, R. Opila, R. W. Collins, N. Winograd, D. L. Allara, "Chemical Effects of Methyl and Methyl Ester Groups on the Nucleation and Growth of Vapor-Deposited Aluminum Films," J. Am. Chem. Soc. 121, 8052 (1999).

[9] J. J. Senkevich, F. Tang, D. Rogers, J. T. Drotar, C. Jezewski, W. A. Lanford, G.-C. Wang, T.-M. Lu, "Substrate-Independent Palladium Atomic Layer Deposition," Chem. Vap. Deposition 9, 258 (2003).

[10] G. L. Fisher, A. E. Hooper, R. L. Opila, D. L. Allara, N. Winograd, "The interaction of vapor-deposited Al atoms with CO2H groups at the surface of a self-assembled alkanethiolate monolayer on gold," Phys. Chem. B 104, 3267 (2000).

[11] J. J. Blackstock, Z. Li, M. R. Freeman, D. R. Stewart, "Ultra-flat platinum surfaces from template-stripping of sputter deposited films," Surf. Sci. 546, 87 (2003).

[12] N. Prathima, M. Harini, N. Rai, R. H. Chandrashekara, K. G. Ayappa, S. Sampath, S. K. Biswas, N. Prathima, M. Harini, N. Rai, R. H. Chandrashekara, K. G. Ayappa, S. Sampath, S. K. Biswas, "Thermal study of accumulation of conformational disorders in the self-assembled monolayers of C8 and C18 alkanethiols on the Au(111) surface," Langmuir 21, 2364 (2005).

[13] M. J. Hostetler, W. L. Manner, R. G. Nuzzo, and G. S. Girolami, "Two-dimensional melting transitions of rod-like molecules analyzed by reflection-absorption infrared spectroscopy," J. Phys. Chem. 99, 15269 (1995).

[14] A. Michaelides and P. Hu, "Softened C–H modes of adsorbed methyl and their implications for dehydrogenation: An ab initio study," J. Chem. Phys. 114, 2523 (2001).

[15] M. Yamamoto, Y. Sakurai, Y. Hosoi, H. Ishii, E. Ito, K. Kajikawa, Y. Ouchi, and K. Seki, "Physisorption of a long-chain n-alkane on Ag(111) surface: an infra-red reflection absorption spectroscopic study," Surf. Sci. 427-428, 388 (1999).

[16] R. A. MacPhail, H. L. Strauss, R. G. Snyder, and C. A. Elliger, "Carbon-hydrogen stretching modes and the structure of n-alkyl chains. 2. Long, all-trans chains," J. Phys. Chem. 88, 334 (1984).

[17] N. P. Kobayashi, C. L. Donley, S.-Y. Wang, and R. S. Williams, "Atomic layer deposition of aluminum oxide on hydrophobic and hydrophilic surfaces," J. Crystal Growth 299, 218 (2007).